Photodeposited Ag-Wires on TiO2 Films

Mills, A., O'Rourke, C., Wells, N., & Andrews, R. (2019). Photodeposited Ag-Wires on TiO2 Films. *Catalysis Today*, *335*, 136-143. https://doi.org/10.1016/j.cattod.2018.10.045

Published in:
Catalysis Today

Document Version:
Peer reviewed version

Queen's University Belfast - Research Portal:
Link to publication record in Queen's University Belfast Research Portal

Photodeposited Ag-Wires on TiO_2 Films

Christopher O'Rourke, Rachel Andrews, Nathan Wells and Andrew Mills*

School of Chemistry and Chemical Engineering, David Keir Building, Stranmillis Road, Belfast, BT9 5AG, UK

e-mail: andrew.mills@qub.ac.uk

Abstract

Highly conducting films of Ag are photodeposited onto commercial self-cleaning glass (Pilkington, Activ™), as well as in-house prepared sol-gel TiO_2 films, using an aqueous solution of $AgNO_3$ containing a sacrificial electron donor, glycerol. Wire tracks are created by irradiating the photocatalytic surface through a stencil, promoting Ag-deposition only on the exposed/irradiated areas. The ability of the Ag-wires to conduct and so heat up the underlying glass is investigated initially for demisting purposes. The photodeposited Ag-wires on Activ™ glass are found to have a resistance of ca. 150 Ω after 2 h irradiation (I = 4 mW cm^{-2}, 352 nm BLB), whereas the Ag-wires on sol-gel film, prepared under the same conditions, are ca. 3 times less resistive (55 Ω). Repeat heating-cooling cycles are achieved by applying a voltage, 12 V, across the Ag wires and demonstrate the robustness of the Ag-wires on Activ™ and sol-gel films, which produce a consistent 20°C, and 40°C, rise in temperature above ambient room temperature, respectively. An Scanning Elen Microscopy study of Ag-particle growth on sol-gel TiO_2 films demonstrates island growth of the Ag-particles, producing Ag 'wires' that are only able to conduct once the Ag 'islands' overlap; typically this is after ca. 9 min of irradiation (I = 4 mW cm^{-2}), with R = 200 kΩ and Ag 'island' particle size = ca. 100 nm. Upon further irradiation, the particles eventually grow sufficiently large that most Ag particles overlap and the resulting Ag wires are highly conducting (R = 55 Ω after 2 h).

Key words: photocatalyst; photodeposition; silver; TiO_2; wires

Introduction

The ever-growing interest in the well-established research area of semiconductor photocatalysis has led to a number of significant commercial products, such as: 'self-cleaning' glass, tiles, concrete, paper, and paint [1-5]. In the vast majority of these products, TiO_2 is the semiconductor of choice. In semiconductor photocatalysis, UV light from a solar or artificial light source is absorbed by the semiconductor to produce electron-hole pairs, which can either recombine in the bulk or surface, of the semiconductor, or react with surface-adsorbed species. In many commercial photocatalytic materials the key photocatalytic reaction is that of the oxidation of an adsorbed organic 'test' pollutant to its mineral form by oxygen, i.e. [6,7].

$$\text{Organic} + O_2 \xrightarrow[h\nu \geq E_{bg}]{\text{semiconductor}} CO_2 + H_2O + \text{mineral acids} \quad (1)$$

where, hν is the energy of the incident light which must be greater than or equal to the bandgap energy of the semiconductor photocatalyst, E_{bg}. The photocatalysed oxidation of pollutants by oxygen, as exemplified by reaction (1), is the basis of the 'self-cleaning' and 'air-purifying' features claimed by most commercial photocatalytic materials. Semiconductor photocatalysis has been most employed for wastewater treatment [8,9], air purification [10,11] and disinfection [12,13], but has has been used (usually in non-aqueous solution) to promote the selective oxidation and reduction of organic substrates [14,15].

In research, although not usually in commercial products, a popular method of improving the performance of semiconductor photocatalysts in the above processes and applications is to use metal/metal oxide co-catalysts deposited on the surface of the semiconductor photocatalyst. This also opens up other avenues of application such as the use of semiconductor photocatalysts for water splitting, Surface Enhanced Raman and Resonance Raman and plasmonic photocatalysis. In many cases the deposition of metal/metal oxide nanoparticles onto the surface of the semiconductor particles or film is achieved *via* photodeposition [6,7] under anaerobic conditions, i.e.

$$2M^{n+}(aq) + nH_2O \xrightarrow[h\nu \geq E_{bg}]{\text{semiconductor}} \left(\frac{n}{2}\right) O_2 + 2nH^+ + 2M^{\geq 0}(s) \quad (2)$$

where $M^{\geq 0}$ is either the metal (M^o) or metal oxide ($M^{>o}$); in practice both are usually deposited. However, more often than not the metal, commonly Pt, is the desired co-catalyst and is usually photodeposited by adding a sacrificial electron donor to the solution [21], whereupon reaction (2) transforms into:

$$M^{n+}(aq) + nSED \xrightarrow[h\nu \geq E_{bg}]{\text{semiconductor}} nSED^+ + M^0(s) \quad (3)$$

The deposition of the metal nanoparticles such as; Ag [9,12], Au [10,15], Pt [8,10,11], Pd [10], and Ir [14], has – in general – been found to enhance the rates of various photocatalytic reactions in general for a wide variety of semiconductors, not least of which is TiO_2. It is usually suggested that these metal deposits act as: charge carrier centres which suppress the recombination of photogenerated electrons and holes, as well as active sites which facilitate charge-transfer reactions [6,7].

The photodeposition of metals has several advantages over other popular methods of metal deposition, such as: impregnation, chemical reduction, electrodeposition, atomic layer deposition, sputtering and physical mixing. These advantages include the negation of: high temperatures, expensive equipment, and having to apply a potential [7]. Photodeposition also allows good control over particle size and the oxidation state of deposited metal/metal oxide particles, since the rate of reaction can usually be controlled by altering the incident irradiance level and irradiation time. Finally, in the photodeposition method the metal is deposited at the active photocatalyst sites, and not randomly across the surface of the semiconductor photocatalyst.

As well as enhancing the activity of the underlying photocatalyst, the photocatalysed deposition of metals has also been used to create surface metal images and micro- and sub-micro patterns of the metal on the semiconductor's surface, although, somewhat surprisingly, this subject area has not been studied in detail. Indeed, since such work shows that surface metal micropatterns and images on a semiconductor film can be created it seems appropriate to ask if they can be made to conduct, i.e. can semiconductor photocatalysis be used to generate wires? This would appear a particular relevant question given that wires on substrates used in semiconductor photocatalysis, such as glass, are a common feature of car, train and plane windscreens, glass doors on fridges and freezers and any other device where defogging/defrosting is necessary. In addition, they have also been used in display cases in delicatessens to keep food warm [16].

There are several methods used in the manufacture of heated windscreens, none of which are simple and inexpensive. For example, the classic heated rear car windscreens with the clearly visible metal tracks, typically 0.5 mm thick [17], are prepared *via* screen-printing a silver ink [18,19] (composed of silver powder, glass frit, and a polymer) through a 150-250 stainless steel mesh onto the inner surface of the windscreen. The ink is then dried at 150°C before being fired at 625-700°C for 2 to 4 min, followed by cold air tempering [18]. Such windscreens are able to effect a typical surface temperature rise of 16 – 18°C when a potential of 12 V is applied [17].

Advancements have been made in recent years to improve the visibility out of heated rear windscreens with the use of thin tungsten wire, typically 14 – 20 µm, instead of the usual relatively thick, 0.5 mm, silver tracks noted above [20,21]. The tungsten tracks are applied to the polyvinyl butyral (PVB) inner laminating layer of the two sheets of glass used to make up car windscreens. More recent developments, by manufacturers such as Volkswagen, have seen the production of wire-free heated windscreens for 'perfect visibility' [22]. Such windscreens incorporate an extremely thin conductive layer of silver within the laminated glass. Creating such layers does, however, require more complex manufacturing procedures and, therefore, cost; for example, a patent from the Ford Motor Company mentions the use of vacuum metal deposition to create such layers for use in their cars [23].

Overall, despite the common use of wires on glass, e.g. in windscreens, refrigerators and shop displays etc, the manufacture of such products is by no means trivial nor, therefore, inexpensive. So, could semiconductor photocatalysis be sued to make such a product? Certainly it is possible, nowadays, to make very thin films of TiO_2 using a wide variety of techniques, such as CVD, PVD and sol-gel. Indeed, the commercial self-cleaning glass manufactured by Pilkington Glass, Activ™, is made using CVD and typically comprises a 15 nm film of 30 nm diameter particles of anatase TiO_2 [24] Thus, this work aims to create highly conducting wires of silver on commercially available self-cleaning glass (Activ™), as well as in-house prepared sol-gel TiO_2 films, and to evaluate their ability to conduct electricityand so heat up the underlying glass for, initially at least, demisting purposes.

Experimental

Materials

Unless stated otherwise all chemicals were purchased from Sigma Aldrich and used as received. The Activ™ film was a gift from Pilkington Glass NSG. All water used to make the aqueous solutions was doubly-distilled and deionised. The methanol used to make up the $AgNO_3$ solution was purchased from Fisher Chemicals.

TiO_2 sol-gel films

A paste of TiO_2 nanoparticles was prepared using a sol–gel method, the details of which are described in detail elsewhere [25]. Briefly, an aliquot of the precursor solution, titanium(IV) isopropoxide (20 cm^3), was modified through the addition of glacial acetic acid (4.65 g). The TiO_2 was then synthesised *via* the sol–gel process by the subsequent addition of 120 cm^3 of deionised water, containing 1.08 g of nitric acid, to the Ti(IV)/acetic acid solution, so as to generate a dispersion of the hydrous oxide. This dispersion was used to grow colloidal TiO_2 particles hydrothermally, *via* Ostwald ripening, using an autoclave (220°C for 12 h). The resulting precipitated TiO_2 colloidal particles were then re-dispersed using an ultrasonic probe. The dispersion was then rotary evaporated until a weight percent of TiO_2 of 10–12% was achieved and then 50 wt% of polyethylene glycol was added as a binder to help prevent the formation of cracks when casting the paste to produce films. The final product is a white paste, the 'sol-gel paste', which is mayonnaise-like in appearance and texture and, when coated, dries in air to form a clear film of amorphous TiO_2.

Silver deposition on commercial self-cleaning Activ™ glass (Ag-Activ films)

Most examples of the photocatalytic deposition of metals onto semiconductor films or powders [8,10,11,14,15] based on reaction (2), use an aqueous solution of the metal salt, which also contains a sacrificial electron donor, such as methanol or ethanol. It is possible to create wire-like images on a commercial photocatalyst film, such as that on Activ™ glass, by irradiating it through a photomask, however, they are not sharp, due to the leakage through the mask; thus, in order to create well-defined, photodeposited Ag wires, insulating tape, with a stencil of a wire, was used to cover the commercial photocatalytic glass sample, which was then immersed in the silver nitrate photodeposition solution (*vide infra*) and irradiated with UVA light. As well as preventing the UVA light getting through the masked areas, the mask prevents the $AgNO_3$ solution coming into contact with the tape-covered TiO_2, thereby, allowing irradiation of the sample from both above and below. This double irradiation appeared to produce the best conducting films, since, when the sample is only irradiated from above, the Ag deposit formed quickly inhibits the absorption of the UVA light by the underlying TiO_2 layer and so prevents the substantial development of the photodeposited Ag layer.

Throughout this work, unless stated otherwise the Ag photodeposition solution was prepared by adding 0.5 g $AgNO_3$ to 100 mL of a 75:25 v/v mixture of methanol and water, respectively. The masked Activ™ glass slides were placed in a petri dish and sufficient $AgNO_3$ solution added to

completely submerge the samples by ca. 1 cm of solution. The templated, submerged Activ™ glass slides were then irradiated from above and below with UVA from a 15 W 352 nm Sankyo Denki BLB lamp (I = 4 mW cm^{-2}) for 2 h. The latter represents the standard irradiation conditions in all this work unless stated otherwise. Figure 1(a) illustrates photographs of the TiO_2 film before and after the photodeposition of a Ag 'wire' on an Activ™ film.

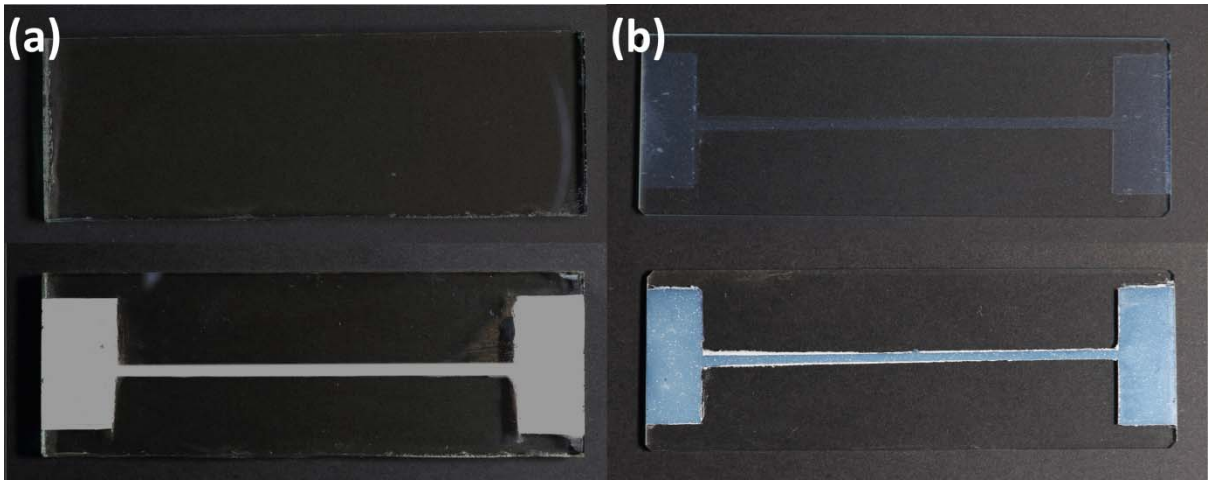

Figure 1 (a) Photographs of Activ™ glass sample before (top) and after Ag-deposition (bottom). (b) Photographs of a sol-gel TiO_2 coated microscope slide before (top) and after Ag-deposition (bottom). Wire width = ca. 1 mm. The pads at either end allow for better contact with crocodile clips

In order to protect the deposited Ag wires from air oxidation/corrosion, i.e. tarnishing, especially when under electrical bias, where they would be hot, a 4 µm thick acrylic coating (RS Pro Clear Acrylic aerosol, PCB Lacquer, 42.6 kV mm^{-1}) was deposited over the whole surface of the glass slide using an acrylic aerosol spray (RS Pro Clear Acrylic aerosol, PCB Lacquer). Note: during the coating procedure, the end pads of the wire (see figure 1(a)) were shielded under a card from the acrylic spray so that the electrical connections could still be made.

Silver deposition on sol-gel TiO_2 (Ag-TiO_2 films)

The masking tape stencil technique used above to create Ag wires on Activ™ glass is only appropriate for photocatalytic films that are sufficiently robust that they cannot be removed when the masking tape is peeled away. Unfortunately, the sol-gel TiO_2 film is not robust enough to withstand this process, therefore, the sol-gel paste itself was cast into the desired shape onto glass slides via a doctor blade technique and a stencil with the same shape as used with Activ™ glass, but this time made out of Scotch® Magic™ tape [25]. A few drops of the TiO_2 sol-gel paste were then pipetted at the top of this Magic™ tape stencil and drawn down the length of the tape using a glass rod, thereby creating a uniform 60 µm thick coat of the TiO_2 sol-gel paste in the shape of the stencil in the Scotch® Magic™ tape. After 30 min, the Scotch tape was removed and the sol–gel film was annealed at 450°C for 30 min with a ramp rate of 10°C min^{-1}. The film was then left overnight to cool slowly inside the furnace to create a final robust, clear coating of anatase TiO_2, approximately 2 µm thick [25], and in the shape of the desired final Ag wire coating.

The shaped TiO_2 coating on glass slide was then placed in a petri dish containing the usual $AgNO_3$ photodeposition solution and irradiated under the same conditions as the Activ™ glass slides for 2 h, *vide supra*. Finally, the final product, the shaped TiO_2 sol-gel film with a Ag-deposited surface, was then coated with a 4 µm thick protective acrylic layer. Figure 1(b) illustrates the appearance of the TiO_2 sol-gel film before and after Ag photodeposition.

Methods

Scanning electron microscope (SEM) images were recorded using a FEI Quanta FEG 250 – Environmental SEM instrument. All photographs were generated using a Canon 7D MKII fitted with a Canon EF 24-70mm f/2.8L II USM lens. The Ag loadings on all the samples were determined by dissolving the metal using concentrated nitric acid followed by Atomic Absorption Spectroscopy (AAS). Unless stated otherwise, all voltages applied across the terminals of the photodeposited Ag wires were provided by an Aim-TTi EL302 Digital Bench Power Supply, 1 Output, 0–30V, 0–2A, 60W. All resistances were measured using an Amprobe 15XP-B multimeter. Thermal images were recorded using a FLIR TG165 Infrared Thermometer. All temperatures were measured using a calibrated thermocouple (Hanna HI-935005) typically positioned ca. 1 mm away from the Ag-wire at the centre of microscope slide.

Results and Discussion

Ag-wire on Activ™ (Ag-Activ) films: initial study

The surface of the Activ™ sample with, and without, a photodeposited wire, see figure 1(a), was studied using scanning electron microscopy and the results of this work are illustrated in figure 2. Thus, figure 2(a) shows an SEM image of the surface of Activ™ glass and reveals that it has a 'cobble-stone' appearance, comprising spherical-shaped TiO_2 particles ca. 32 nm ± 4 nm in diameter, which is consistent with a previous report [24]. It follows that, as the thickness of the CVD deposited layer of TiO_2 is typically ca. 15 nm [24], the surface of the Activ™ glass is covered with flattened hemispheres of TiO_2. The surface of a typical Ag-Activ sample, illustrated in figure 1, is very different, as shown by the SEM image in figure 2(b), an analysis of which suggests an average large Ag particle size is 2.3 µm ± 0.5 µm. The loading of the Ag on the Ag-Activ sample was determined to be ca. 0.4 mg of Ag cm^{-2}. Encouragingly, these Ag-films were found to be conducting and exhibited a resistance of ca. 150 Ω across the length of the 7.6 cm 'wire' illustrated in figure 1. Initially, this observation of conduction appears to contradict what is seen in the SEM, figure 2(b), namely, a field of large, apparently *isolated* Ag particles (2.3 µm). However, a more careful examination of the SEM reveals the surface to comprise many smaller Ag particles (0.2 µm ± 0.5 µm) which are in contact with each other, and so allow the Ag photodeposited film to conduct electricity. A clear demonstration of the conducting nature of the Ag-wire on Activ™ was provided by connecting the latter to a 9 V battery and 455 nm LED, as illustrated in figure 2(c).

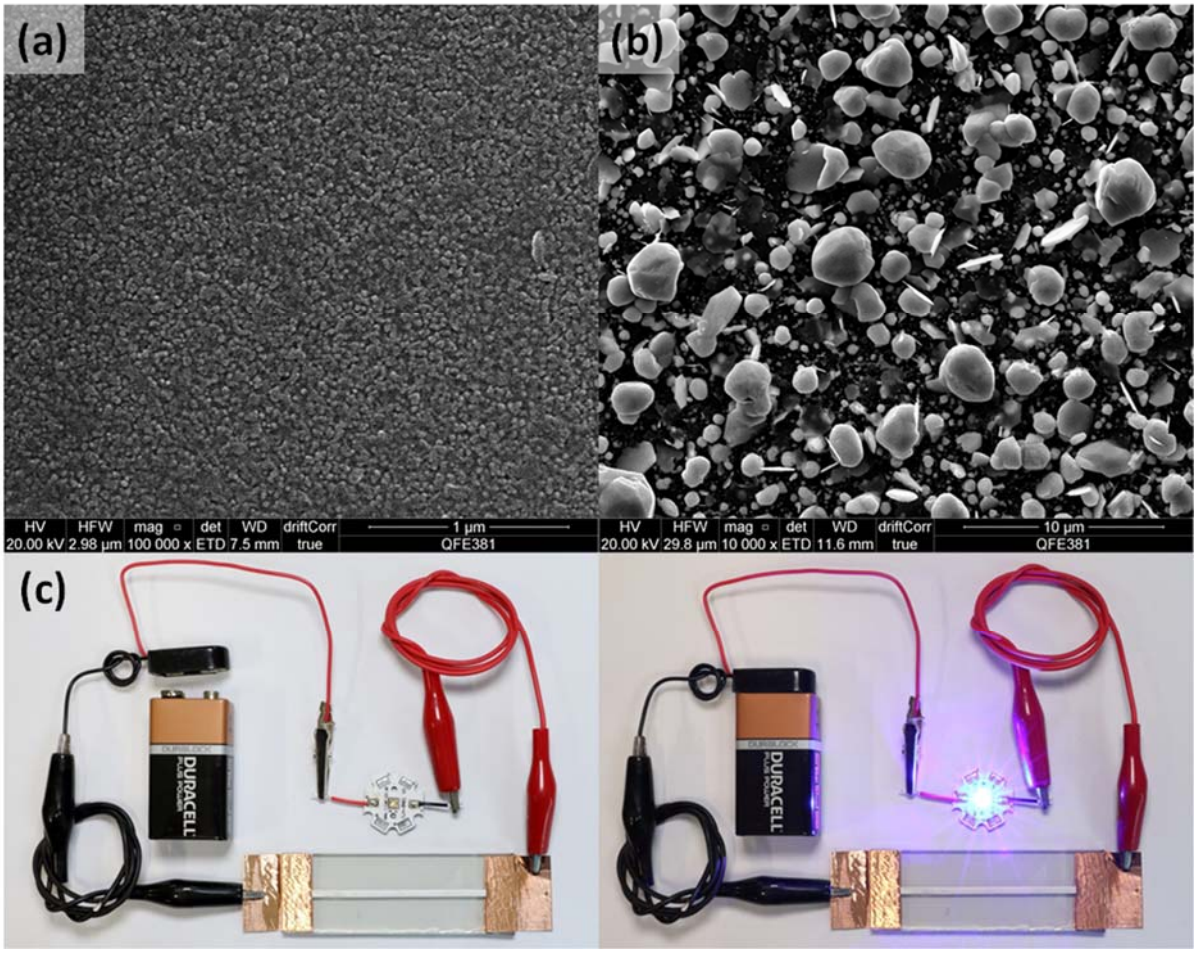

Figure 2 (a) SEM image of the surface of Activ™ at 100,000 times magnification. (TiO_2 particle size = 32 nm ± 4 µm). **(b)** SEM image of the surface of a Ag-Activ at 10,000 times magnification and (Ag particle size = 2.3 µm ± 0.5 µm,). **(c)** Photographs of a Ag-Activ (R = 150 Ω) as part of a circuit to light an LED (OSLON+ PowerStar Deep Blue 455 nm). The left image shows the 9V battery disconnected, and the image on the right shows the completed circuit illuminating the LED (I = 60 mA).

As the Ag-Activ film is conducting it follows that by passing a current through the Ag wire it should be possible to heat up the underlying glass substrate, since all conductors generate heat because they offer a resistance to the flow of electrons so that some of the kinetic energy of the electrons is converted to thermal energy. In order to demonstrate this heating effect, in one set of experiments, the Ag-Activ glass sample, illustrated in figure 1(a), was covered with a thin layer of frost (0.26 mm thick) by placing it directly above a Dewar of liquid nitrogen. The frosted Ag-Activ glass sample was then defrosted, whilst still being held in place above the Dewar, by applying 12 V across the terminals of the Ag wire on the Ag-Activ glass sample. The subsequent defrosting of the glass was monitored photographically and the results of this work are illustrated in figure 3(a). This series of photographs, taken at 4 minute intervals, shows the gradual defrosting of the glass occurs while the Ag-Activ sample remains above the liquid nitrogen Dewar. Other work showed that the temperature that the Ag-Activ sample eventually reached was 26°C after 24 min.

In order to determine what temperatures this system could reach under ambient conditions, the same Ag-Activ sample was subjected to three voltage on/voltage off cycles under room temperature conditions, whilst the temperature of the glass near the wire (1 mm from wire in centre of slide) was monitored continuously. The results of this work are illustrated in figure 3(b) and demonstrate the reversibility and robustness of the Ag wire on the Ag-Activ glass sample, since the profiles show no evidence of a drop in the performance over 3 heating/cooling cycles ($V_{applied}$ = 12 V, I = 80 mA). Under the latter conditions, in each cycle the Ag wire is able to produce a temperature rise of ca. 20°C.

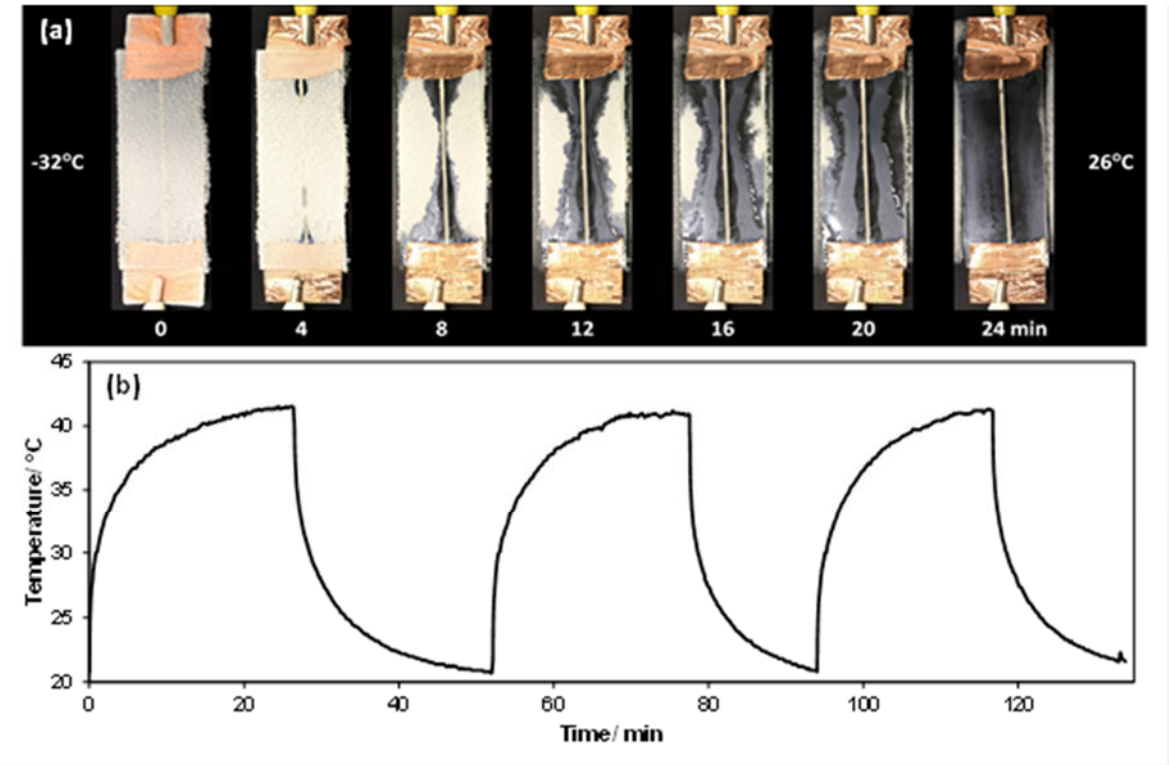

Figure 3 (a) A series of photographs showing the defrosting ability of a Ag-Activ (R (Ag-film) = 150 Ω, I = 80 mA), when a potential of 12 V was applied over a 24 min period, raising the temperature from -32°C to 26°C. **(b)** Repeat heating and cooling cycles under ambient conditions, showing little/no evidence of degradation of the Ag- Activ ($V_{applied}$ = 12 V, I = 80 mA); initial ambient temperature = 20.8°C; typical maximum temperature = 41.3°C.

Although the performance of the Ag-Activ film looks promising as a possible method for producing heated glass, the Ag particles do not adhere well to the relatively smooth, thin 15 nm thick, non-porous TiO_2 surface. In addition, the film is very resistive (R = 150 Ω), which limits the current that can flow for a fixed (in this case 12 V) applied voltage, which in turns limits the temperature rise that can be produced. Thus, the focus of this work turned to testing a different type TiO_2 film, namely a thick (2 μm) mesoporous sol-gel film, which might be expected to produce a more conducting photodeposited Ag film.

Ag-wire on a TiO_2 sol-gel film (Ag-TiO_2): initial study

The photodeposition of Ag on a thick mesoporous TiO_2 sol gel film, here referred to as the 'Ag-TiO_2' film, to distinguish it from the previous 'Ag-Activ' film, should result in a more conductive, robust Ag wire since such a film should allow the growth of Ag particles not only on the surface (as with Activ™) but also in the mesopores of the TiO_2 film, which should generate more routes for electrical conduction due to the greater network of Ag particles.

As before, the surfaces of the TiO_2 film and the photodeposited Ag were probed using SEM and the results of this work are illustrated in figure 4. The SEM illustrated in figure 4(a) is that of a typical 'naked' TiO_2 sol-gel film (see figure 1) and reveals a mesoporous surface comprising small TiO_2 particles with an average size of 29 nm ± 5 nm. In contrast, the SEM of the surface of Ag-TiO_2 film , illustrated in figure 4(b), reveals a coverage of very much larger Ag particles, typically 0.3 μm ± 0.05 μm, although very much smaller, and more homogeneous, than those found on the Ag-Active film, see figure 2(b), i.e. 2.3 μm. The surface thickness of the Ag film on the Ag-TiO_2 was found to be ca. 0.5 μm ± 0.1 μm, which was about a quarter of that of the Ag film on the Ag-Activ film; however, Energy Dispersive X-Ray Spectroscopy (EDS) analysis confirmed that the Ag particles were embedded throughout the TiO_2 layer, a feature that is not possible for the Ag-Activ film, since in the latter case the underlying TiO_2 film is not porous. The loading of Ag was determined (from AAS) to be ca. 0.15 mg of Ag cm^{-2}, i.e. ca. 2.7 times less than that on the Ag-Activ film. Most importantly, from the SEM image illustrated in figure 4(b) it is clear that the photodeposited Ag particles are in close proximity to each other and, therefore, it is perhaps not surprising to note that the measured resistance of the Ag-wire on a Ag-TiO_2 film, illustrated in figure 1(b),was only 55 Ω, i.e. ca. 3x lower than the equivalent (in terms of width and length and method of preparation) Ag-wire on Activ™ glass, i.e. that illustrated in figure 1(a).

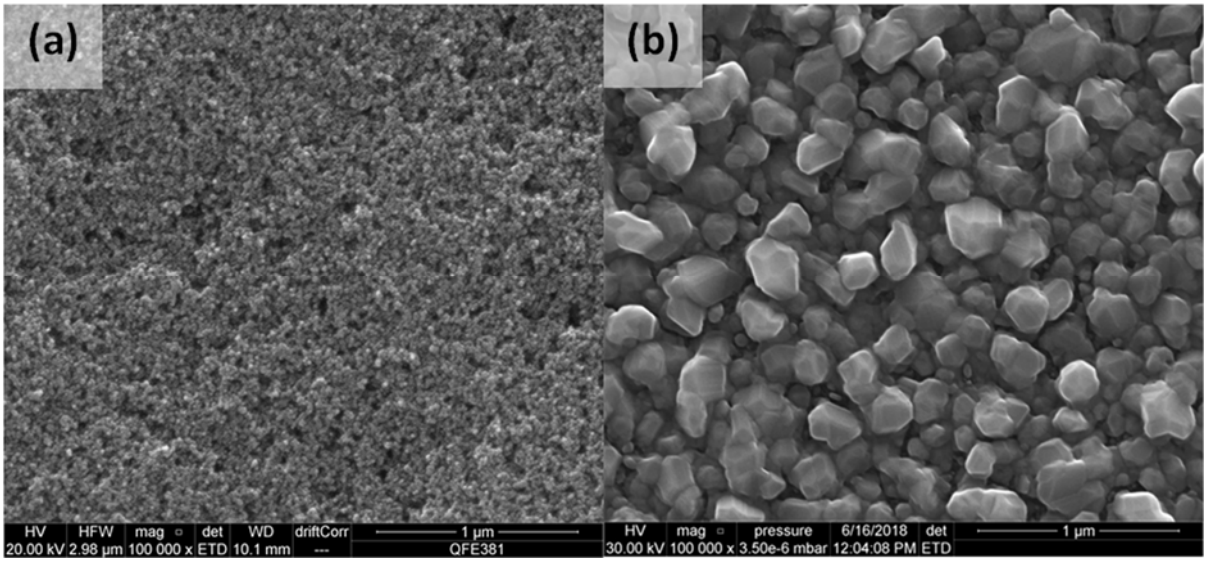

Figure 4 (a) SEM image of the surface of a sol-gel TiO_2 film (100,000 x mag.) (TiO_2 particle size = 29 nm ± 5 nm). **(d)** SEM image of the surface of a Ag-deposited coating on a sol-gel TiO_2 film (100,000 x mag.) (Ag particle size = 0.3 μm ± 0.05 μm).

The ability of the Ag-TiO_2 film to defrost glass was then demonstrated using the same procedure as before for producing the frost, i.e. placing the slide above a Dewar of liquid nitrogen and then applying 12 V across the wire. The results of this work are illustrated by the photographs in figure 5(a) which show the Ag-TiO_2 film is able to much more rapidly defrost the glass (1.4 min compared to 24 min) than the Ag-Activ glass under otherwise the same conditions.

The reusability/robustness of the Ag-TiO_2 film was also assessed by applying 12 V for 5 min and then allowing it to cool back down to ambient temperature, before repeating the cycle a further 2 times. The results of this study are illustrated in figure 5(b) and reveal no evidence of any drop in the performance of the wire over the 3 cycles, which gives a consistent rise in temperature of ca. 44°C after 5 min at 12 V.

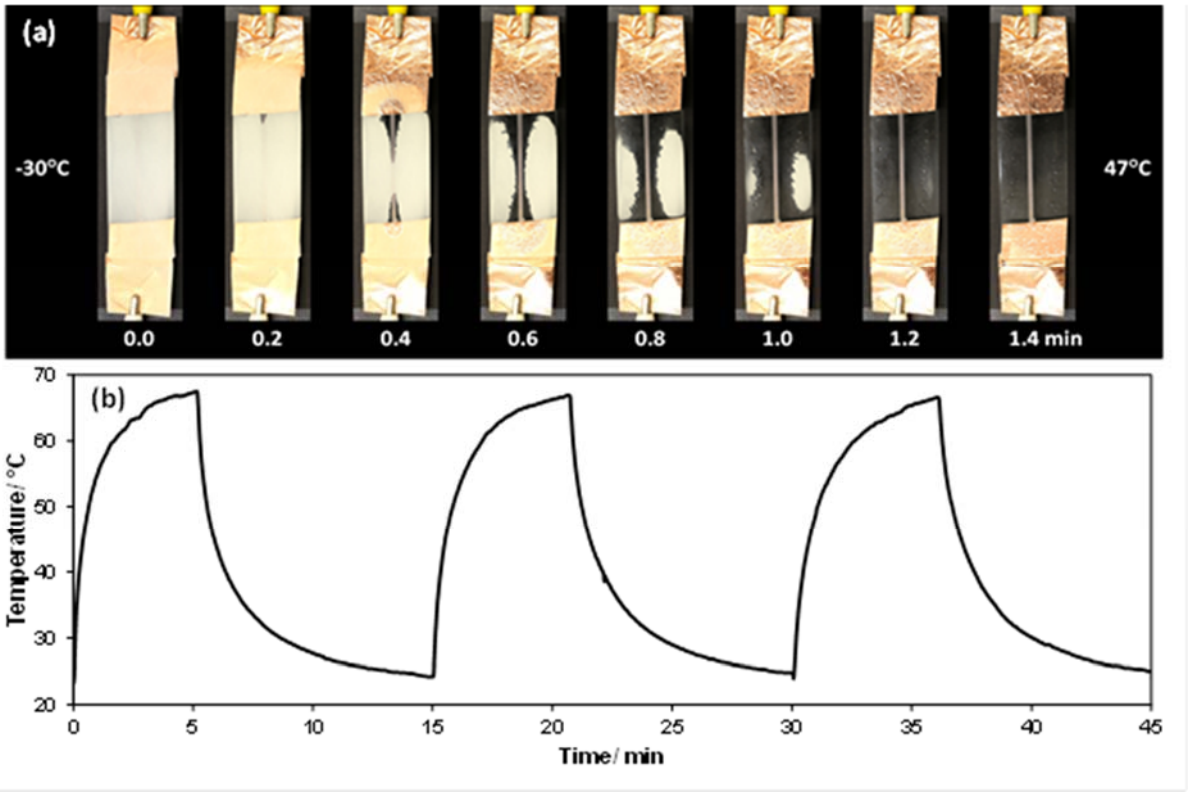

Figure 5 (a) A series of photographs showing the defrosting ability of a Ag-TiO_2 wire (R (Ag-wire) = 55 Ω, I = 200 mA), when a potential of 12 V was applied over a 1.4 min period, raising the temperature from -30°C to 47°C. **(b)** Repeat heating and cooling cycles under ambient conditions, showing little/no evidence of degradation of the Ag-TiO_2 wire ($V_{applied}$ = 12 V, I = 200 mA).); initial ambient temperature = 23.2°C; typical maximum temperature = 67.3°C.

This work shows that the Ag-TiO_2 film is much more conducting, and thus more effective in defrosting glass, than the Ag-Activ film. In addition, the Ag-TiO_2 film is more robust, as the Ag particles are smaller and embedded in the mesoporous structure of the TiO_2 film. As a result, the Ag-TiO_2 film was investigated further.

Ag-TiO_2: further heat study work

Thermal imaging was used to allow the temperature distribution in the TiO_2 sol-gel film, and supporting glass substrate, to be monitored, as well as that of the Ag wire on a Ag-TiO_2 film, as a function of time after a voltage was applied across the Ag wire. Figure 6(a) shows the change in thermal image of the Ag-TiO_2 film as a function of time after a potential of 12 V was applied across the Ag wire (I = 0.2 A, R = 55 Ω). Initially at an ambient temperature of 24.8°C, the wire heats up rapidly and that within 5 – 6 min the glass slide follows suit, reaching a localised temperature next to the wire of up to 70.5°C.

In a more detailed study of the electrical heating of the Ag-TiO_2 film, the temperature versus time profiles were recorded for a range of applied voltages across the Ag wire of 3 – 12 V and some of the results of this study are illustrated in figure 6(b); note: in this work room temperature was ca. 21°C. From this study, the maximum change in temperature, ΔT_{max}, i.e. the different between the initial room temperature and the final plateau temperature, was determined for the different applied voltages and used to generate a plot of ΔT_{max} vs power (I x $V_{applied}$), which yields a straight line as shown in figure 6(c). This plot suggests that for the Ag-TiO_2 film, the electrical power, P, is related to the temperature change, ΔT, via:

$$P = K\Delta T \quad (3)$$

where K is 0.062 W K^{-1} (or 14.9 W m^{-2} K^{-1}) and provides a measure of the glass sample to radiate heat. A similar calculation for the Ag-Activ sample generates a value of K = 0.048 W K^{-1} (10.5 W m^{-2} K^{-1}).

The lower resistance of the Ag-TiO_2 film, compared to the Ag-Activ, allows the former system to pass a higher current (200 mA for Ag-TiO_2 cf. 80 mA for Ag-Activ), and so is able to produce a greater temperature change of ca. 40°C at 12 V, compared with the 20°C rise observed for the Ag-Activ under otherwise the same conditions. Note, however, that because both the Ag-Activ and Ag-TiO_2 samples are approximately the same size, they are likely to lose heat at similar rates. As a consequence it might be expected that the steady state temperature change, ΔT_{max}, observed for the Ag-Activ sample (20°C for a power of 1.0 W), would be similar to that observed for the Ag-TiO_2 film for the same power (14°C for a power of 1.0 W), as appears to be the case and as illustrated in figure 6(c) by the black and open circle data points at 1 W recorded for the Ag-TiO_2 and Ag-Activ films, respectively.

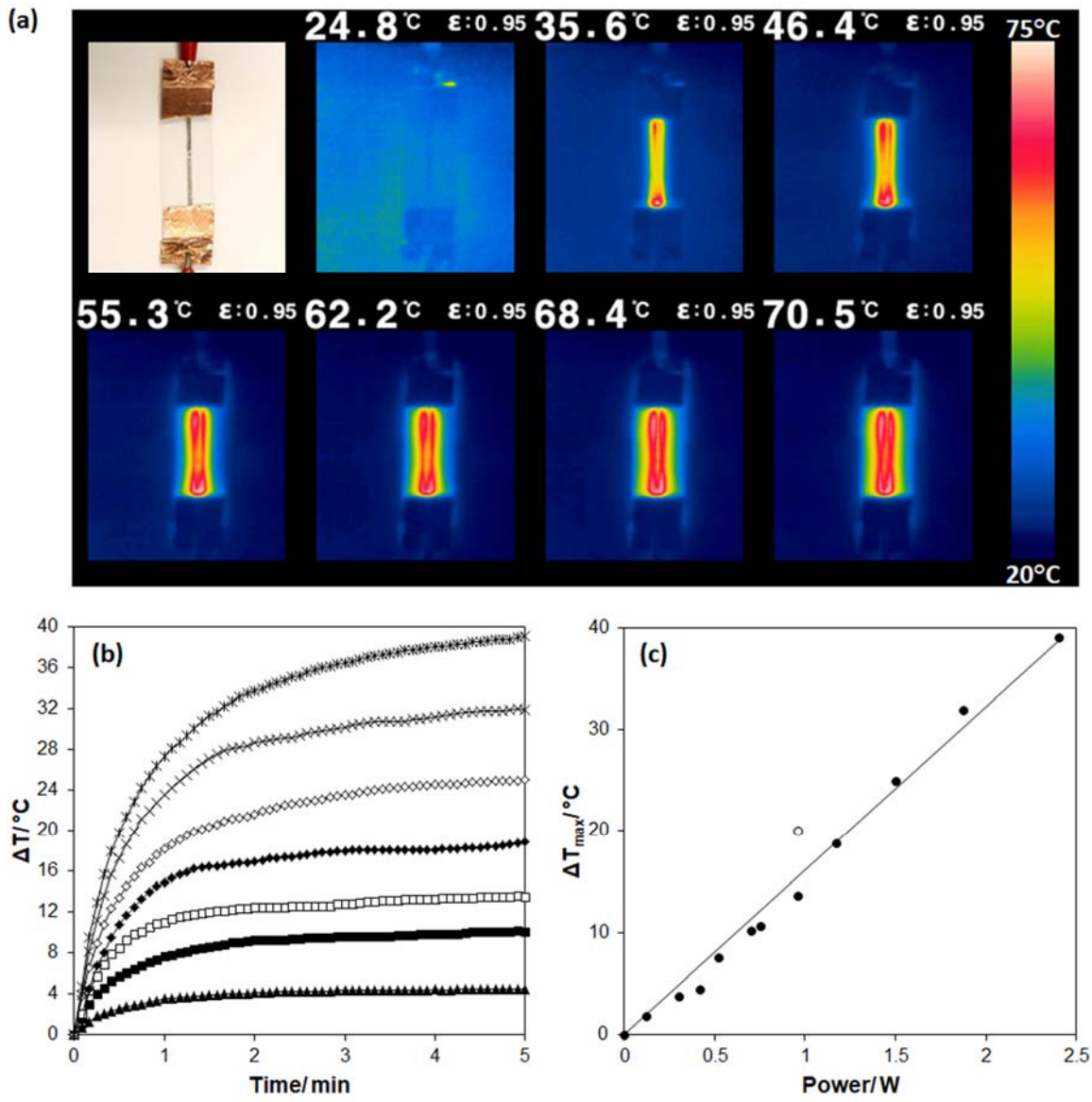

Figure 6 (a) Photograph of a Ag-TiO_2 wire with copper tape tabs to allow easy connection to a power supply. Some of the thermal images taken at 1 min intervals using a FLIR TG165 Infrared Thermometer when a potential of 12 V was applied (I = 0.2 A, R = 55 Ω) **(b)** A plot of the change in temperature as a function of time for a range of applied potentials (Top to bottom: 12, 11, 10, 9, 8, 7, and 6 V) **(c)** A plot of the maximum temperature attained for each applied potential as a function of power (current x voltage). The open white circle represents the performance of the Ag-Activ film from the data in figure 3(b).

The above work also shows that the simple Ag-TiO_2 film is able to produce a wide range of different temperature changes in the supporting glass substrate within a few minutes of a voltage being applied, which may prove useful in a number of applications, not least of which will be as a means to defrost glass surfaces.

Ag-TiO_2: Ag particle growth

Finally, a study of the Ag particle growth was conducted in which the Ag- TiO_2 sol-gel films were subjected to the typical deposition procedure, I = 4 mW cm^{-2} (352 nm BLB), but for a range of different irradiation times (5 – 120 min). The resistances of all the different photodeposited Ag-films produced from this work were measured and plotted as a function of UVA irradiation time and the results of this work are illustrated in figure 7(a). These results show that despite the rapid formation, i.e. within a few minutes of irradiation, of an intense brown/black colour, as the Ag photodeposits onto the TiO_2 sol-gel film, the Ag film does not appear to conduct until ca. 9 min into the photodeposition process, and even then it is highly resistive, i.e. ca. 200 kΩ. The intense colour is most probably due to the formation of seed metal particles dispersed throughout the TiO_2 film with diameters of 2 – 4 nm, which is not uncommon in the metal photodeposition process using an alcohol-based SED [7]. The presence of Ag throughout the TiO_2 and across its surface, at this early stage in the deposition process, was confirmed by EDS. Although the detection of the small seed Ag particles was beyond the resolution capacity of the SEM used in this work, as the irradiation process continued, SEM image analysis of the samples first (after 5 min irradiation) revealed the formation of small (79 nm), unconnected Ag particles which then grew into bigger, more connected particles, as the UV exposure time was increased, as illustrated in figure 7(b). Thus, after 5 min UV irradiation (R = ∞) there are only small 79 nm Ag particles, distributed far apart from each other and so not able to effect electrical conductivity, whereas after 12 min irradiation, much larger (130 nm) particles are formed, with smaller (49 nm) particles littered in-between them, which help facilitate conduction (R = ca. 800 Ω). Upon even further irradiation, e.g. after 120 min, the particles eventually grow large enough (295 nm) that they overlap considerably with each other and so produce very conductive films (R = ca. 55 Ω after 120 min).

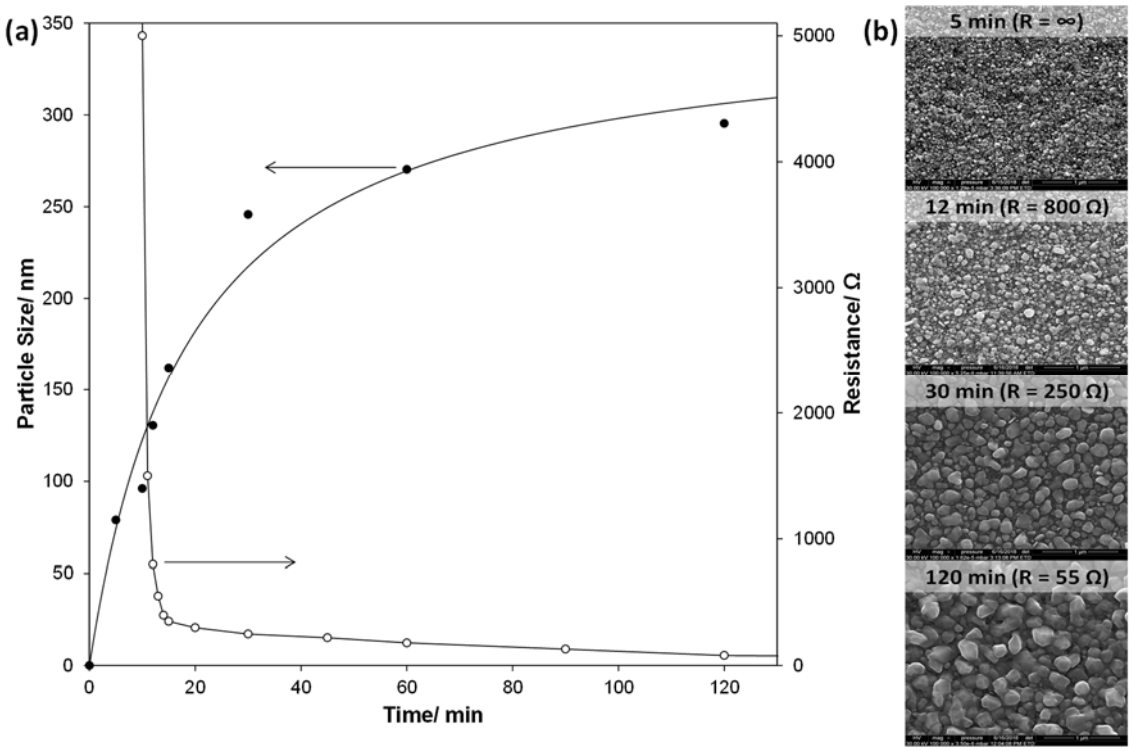

Figure 7 (a) Plot of Ag particle size on sol-gel TiO_2 (●) and the corresponding film resistance (○) as a function of irradiation time. **(b)** SEM images showing the Ag particle growth over time.

The results of this work show that with Ag-TiO_2 films, photodeposition produces Ag metal island growth and that only when the metal particles are above a critical size (ca. 100 nm) do the Ag films conduct and with further irradiation the degree of metal island overlap increases and the resistivity of the film decreases.

Conclusions

Highly conducting Ag-wires can be easily photodeposited, using a $AgNO_3$ solution using ethanol as the sacrificial electron donor, onto commercial self-cleaning glass (Activ^{TM}) as well as in-house prepared sol-gel TiO_2 films. The Ag-Activ film is less conducting (resistances: 150 and 55 Ω for the Ag-Active and Ag-TiO_2 film, respectively) and less robust than the Ag-TiO_2 sol-gel film. For either photodeposited Ag 'wires', when an electrical potential, typically 12 V, is applied, both the wire and surrounding substrate heat up and enough heat is produced to defrost glass cooled initially to ca. -32°C, although this effect is much more significant for the Ag-TiO_2 film since, the change in temperature, ΔT, is 79^{o}C compared to 58^{o}C, since it is 3 times more conducting that the Ag-Activfilm. . This effect can be repeated many times without deterioration. Further work carried out on the Ag-TiO_2 film shows that ΔT is proportional to power in (i.e. current x voltage) and that conduction of the Ag-TiO_2 film only occurs once the Ag particles have grown to a sufficient size and number that they are in contact with one another. The conducting nature of photodeposited metal films on TiO_2 have not, to our knowledge, been studied before and may open up a number of significant, new applications, not least of which would be their use for making heated glass or ceramics, where defrosting or defogging is necessary, such as; car windscreens, glass doors on fridges/freezers, and display cases in delicatessens.

References

[1] Pilkington, http://www.pilkington.com, accessed: June 2018.

[2] TOTO, http://www.toto.com.hk, accessed: June 2018.

[3] Italcementi Group, http://www.italcementigroup.com, accessed: June 2018.

[4] Mitsubishi Paper Mills, https://www.mpm.co.jp/eng/rd/field/functional-material.html, accessed June 2018.

[5] STO, http://www.sto.co.uk, accessed: June 2018.

[6] M. I. Litter, Heterogeneous photocatalysis: Transition metal ions in photocatalytic systems, Appl. Catal. B 23 (1999) 89–114.

[7] K. Wenderich, G. Mul, Methods, Mechanism, and Applications of Photodeposition in Photocatalysis: A Review, Chem. Rev. 116 (2016) 14587−14619.

[8] M. S. Hamdy, W. H. Saputera, E. J. Groenen, G. Mul, A novel TiO_2 composite for photocatalytic wastewater treatment, J. Catal. 310 (2014) 75–83.

[9] S. Parastar, S. Nasseri, S. H. Borji, M. Fazlzadeh, A. H. Mahvi, A. H. Javadi, M. Gholami, Application of Ag-doped TiO2 nanoparticle prepared by photodeposition method for nitrate photocatalytic removal from aqueous solutions, Desalin. Water Treat. 51 (2013) 7137–7144.

[10] N. S.Kolobov, D. A. Svintsitskiy, E. A. Kozlova, D. S. Selishchev, D. V. Kozlov, UV-LED photocatalytic oxidation of carbon monoxide over TiO2 supported with noble metal nanoparticles, Chem. Eng. J. 314 (2017) 600–611.

[11] H. Einaga, M. Harada, S. Futamura, T. Ibusuki, Generation of Active Sites for CO Photooxidation on TiO_2 by Platinum Deposition, J. Phys. Chem. B 107 (2003) 9290−9297.

[12] I. Piwonski, K. Kadzioła, A. Kisielewska, K. Soliwoda, M. Wolszczak, K. Lisowska, N. Wronska, A. Felczak, The effect of the deposition parameters on size, distribution and antimicrobial properties of photoinduced silver nanoparticles on titania coatings, Appl. Surf. Sci. 257 (2011) 7076–7082.

[13] J. Prakash, S. Sun, H. C. Swart, R. K. Gupta, Noble metals-TiO_2 nanocomposites: From fundamental mechanisms tophotocatalysis, surface enhanced Raman scattering and antibacterial applications, Appl. Mater. Today 11 (2018) 82–135.

[14] W. Feng, G. Wu, L. Li, N. Guan, Solvent-free selective photocatalytic oxidation of benzyl alcohol over modified TiO2, Green Chem. 13 (2011) 3265–3272.

[15] M. C. Hidalgo, J. J. Murcia, J. A. Navío, G. Colón, Photodeposition of gold on titanium dioxide for photocatalytic phenol oxidation, Appl. Catal. A 397 (2011) 112–120.

[16] Applience Design, https://www.appliancedesign.com/articles/91372-heating-elements-conductive-clarity-july-2008, accessed: June 2018.

[17] Hiroshi Nakashima, Hiroshi Nagaiwa, Akihiko Matsumoto, Arrangement of heating strips of defogger on vehicle window glass, US6137085A, 2000.

[18] DuPont, http://www.dupont.com/content/dam/dupont/products-and-services/electronic-and-electrical-materials/documents/prodlib/788X.pdf, accessed: June2018.

[19] Johnson Matthey, http://www.glassmatthey.com/automotive/silver-paste, accessed: June2018.

[20] Hamacher Maschinenbau GmbH, http://www.hamacher-maschinenbau.de/en/hotlineglass/, accessed: June2018.

[21] Tyneside Safety Glass, https://tynesidesafetyglass.com/products/heated-glass, accessed: June2018.

[22] Volkswagen, https://www.volkswagen-media-services.com/en/detailpage/-/detail/Perfect-visibility-with-no-heating-wires--the-climate-windscreen-from-Volkswagen/view/4487024/7a5bbec13158edd433c6630f5ac445da, accessed: June2018.

[23] Kevin J. Ramus, Method for making a part of an electrically heated windshield assembly, US4815198A, 1989.

[24] A. Mills, A. Lepre, N. Elliott, S. Bhopal, I. P. Parkin and S.A. O'Neill, Characterisation of the photocatalyst Pilkington Activ™: a reference film photocatalyst?, J. Photochem. Photobiol. A: Chem. 160 (2003) 213-224.

[25] A. Mills, N. Elliott, G. Hill, D. Fallis, J. R. Durrant and R. L. Willis, Preparation and Characterisation of novel thick sol-gel titania film photocatalysts, Photochem. Photobiol. Sci. 2 (2003) 591−596.